

Role of eddies on controlling total and size-fractionated primary production in the Bay of Bengal

V.V.S.S. Sarma*, M. Chopra, D.N. Rao, M.M.R. Priya, G.R. Rajula, D.S.R Lakshmi, V.D. Rao

CSIR-National Institute of Oceanography, Regional Centre, 176 Lawsons Bay Colony,
Visakhapatnam-530 017, India

*Corresponding author

Abstract

In order to examine the role of eddies on total and size-fractionated primary production, two cyclonic (CE), one anticyclonic (ACE) and no-eddy (NE) regions were sampled in the BoB during pre-summer monsoon (June 2019). The upper ocean is strongly stratified due to freshwater discharge from major rivers. Low (high) nutrients concentrations were noticed in the ACE (CE) regions due to convergence (divergence). Prominent existence of deep Chlorophyll-*a* maximum (DCM) was observed and its depth is governed by mixing associated with eddies. High concentration of zeaxanthin and fucoxanthin was observed in the upper 50m and DCM respectively. The dominant contribution of picoplankton biomass (40-80%) to total phytoplankton biomass was observed in the photic zone whereas micro and nanoplankton contributed between 10 and 30%. The photic zone integrated total primary production was higher in the CE and NE than ACE regions associating with higher nutrients in the former than latter region. The primary production by microphytoplankton was higher in the CE and NE than ACE regions. Higher picophytoplankton production was observed at depth below 10 m from surface (10-80%) than nano and microphytoplankton (1-30%). The microphytoplankton production was higher in the CE ($164 \pm 16 \text{ mgC m}^{-2} \text{ d}^{-1}$) than ACE ($60 \pm 26 \text{ mgC m}^{-2} \text{ d}^{-1}$) due to availability of nutrients in the former region resulted from upwelling of subsurface waters. The photic zone integrated total and microphytoplankton primary production displayed linear relation with nutrients (nitrate and phosphate) and inverse relation was observed with picophytoplankton suggesting that the availability of nutrients due to eddy-driven mixing determined the contribution of primary production by different size classes. This study suggests that eddy-driven nutrients increased contribution of primary production by microphytoplankton leading to enhanced export production under CE in the BoB and therefore, these regions can be considered as an efficient regions of carbon sequestration for the atmospheric CO₂. More than 30 eddies form every year with life time of 3-6 months and its impact on sinking carbon fluxes and atmospheric CO₂ sequestration in the BoB needs evaluation using numerical modelling.

1. Introduction

Eddies are generally formed by baroclinic and barotropic instabilities. In the case of BoB, local Ekman pumping, remote forcing from equatorial Indian Ocean and internal instability together play important role in the formation of eddies (Cheng et al., 2018). The coastal poleward propagating Kelvin waves along the eastern boundary of the BoB radiate Rossby waves towards west into the interior Bay (Chatterjee et al., 2017). Due to interaction with the coastal currents, these Rossby waves generate weaker baroclinic instabilities leading to formation of eddies (Chen et al., 2012; Cheng et al., 2013; Chatterjee et al., 2017; Cheng et al., 2018). In addition to this, Rossby waves are significantly altered by the Andaman Nicobar Islands and increase eddy activity in the BoB (Cheng et al., 2018; Mukherjee et al., 2019).

The primary production in the Bay of Bengal (BoB) is considered to be low due to weak nutrients supply through vertical mixing, cloud cover and turbidity (Gomes et al., 2000; Madhupratap et al., 2003; Gauns et al., 2005). Large spatial variability in primary production was reported in the BoB (89 to 221 mgCm⁻²d⁻¹; Gauns et al. (2005), however, potential reasons for such variability is not explained. Doubling of primary production due to nutrients injection in cyclonic eddies (CE) (Kumar et al., 2004) resulting in increase in f-ratio is reported than no-eddy (NE) region in the BoB (Sherin et al., 2018; Sarma et al., 2019a). Increase in sinking biogenic carbon fluxes under the CE was found in the BoB (Vidya and Kumar, 2013) and attributed to possible increase in primary production caused by divergence of waters. The sinking carbon fluxes in the BoB to sea bottom are higher than highly productive Arabian Sea and it is attributed to ballast of organic matter in association with river-borne mineral particles (Ittekkot et al., 1991). Recently Anand et al. (2017) reported low sinking carbon fluxes at 100 m depth in the BoB and attributed to possible primary production by picophytoplankton leading to decomposition of organic matter within the photic zone itself.

Waga et al. (2019) reported that mesoscale eddies modify size structure of the phytoplankton with large cell sizes in the eutrophic CEs and oligotrophic ACEs. Waite et al. (2019) noticed that equal productivity per unit Chlorophyll-a (P_B) in both cyclonic (CE) and anticyclonic (ACE) whereas depth-integrated primary production is greater in the former than latter regions. It was further noticed that dinoflagellates were dominant in CEs and diatoms in the ACEs compared to subtropical front in the south-eastern Indian Ocean (Waite et al., 1992; 2007; 2019; Thompson et al., 2007). Thompson et al. (2007) noticed higher primary production by diatoms in the ACEs whereas contribution by nano and picoplankton dominated in the CEs in the subtropical Indian Ocean. Nevertheless, the response of size classes is depended on the availability of nutrients and mixing conditions within the eddies. The sinking carbon fluxes below the photic zone is governed by the size and density of

phytoplankton, therefore, primary production by microplankton may sink faster than picophytoplankton (Suess et al., 1980; McDonnell et al., 2012; Omand et al., 2020). Sherin et al. (2018) reported that >70% of the phytoplankton biomass is contributed by picophytoplankton due to low nutrients concentrations in the BoB. Loganathan et al. (2019) noticed that unique ecosystem exists in the eddies compared to NE region in the BoB. Therefore, concentrations of nutrients, phytoplankton composition and contribution of primary production by different size classes are expected to be different from that of outside and it is important to evaluate their role on carbon sequestration in the BoB.

In addition to the nutrients limitation, light is reported to be strong controlling factor for phytoplankton biomass and primary productivity due to suspended particulate matter (SPM) load through river discharge and thick cloud cover over the Bay (Radhakrishna et al., 1978; Gomes et al. 2000; Madhu et al., 2006; Paul et al., 2007; 2008; Jyothibabu et al., 2008; Kumar et al., 2010). Qasim (1977; 1982) observed absence of photoinhibition in the phytoplankton in the surface waters of the BoB due to intense cloudcover during summer monsoon (June to September). Gomes et al. (2000) reported low biomass normalized primary production during summer monsoon due to severe light limitation of primary production resulting in less photosynthetic efficiency in the BoB. Interestingly the role of light on primary production was hypothesized based on atmospheric cloud measurements and SPM as photosynthetic active radiation (PAR) was never measured. Recently, Jyothibabu et al. (2018) observed that increase (decrease) in phytoplankton biomass in the upper 40 m of water column is associated with cloudy (sunny) sky during summer monsoon indicating strong role of light on distribution of phytoplankton in the BoB. The objective of this study is to 1) evaluate role of eddies on source of nutrients and primary production, 2) examine the impact of eddies on variability of primary production by different size classes of phytoplankton and 3) estimate the role of light, suspended particulate matter (SPM) and nutrients on limiting primary production in the BoB during summer monsoon.

2. Material and methods

2.1. Study area and sampling

The northeastern Indian Ocean (the Bay of Bengal; BoB) is covered by landmasses in three directions and opened to the south Indian Ocean in the south. It receives significant amount of fresh water from major rivers, such as the Ganges, Brahmaputra Godavari, Mahanadi etc ($1.6 \times 10^{12} \text{ m}^3 \text{ y}^{-1}$; Unger et al., 2003) and sediment (1.1×10^9 tonnes) during summer (June to September) (Milliman and Syvitski, 1992; Milliman and Meade, 1983). The river discharge is a source of nutrients to the

BoB (Krishna et al., 2015) and most of the riverine nutrients are utilized within 10-20 km from the coast (Sarma et al., 2013). Both river runoff and precipitation peaks during summer monsoon resulting in strong stratification that inhibits vertical mixing of nutrients to surface. More than 30 eddies (CE and ACE) forms in the BoB due to local Ekman pumping, remote forcing from equatorial Indian Ocean and internal instability together play important role to the formation of eddies (Chen et al., 2012; Cheng et al., 2018). The formation of eddies and their physical characteristics are well understood in the BoB, however, the importance of biogeochemistry of eddies are less understood in the BoB.

This study was conducted on board *O.R.V. Sagar Nidhi* (Cruise No. SN142) during summer monsoon (11-29 June 2019) in the western and central BoB. The aim of this cruise was to sample within CE, ACE and no-eddy (NE) region to examine the variability in physico-biogeochemical characteristics of the water column, a total of 18 stations were occupied for collection of hydrographic parameters in the upper 100 m and incubation of primary production (both total and size-fractionated) was conducted at 14 stations (Fig. 1; shown as white circles). Seawater samples from standard depths were collected using Niskin bottles (10L capacity) fixed to a rosette, along with conductivity-temperature-depth, (CTD, 19 Plus, SeaBird Electronics, USA) sensors. The detection limits for temperature, salinity, and pressure are 0.001°C, 0.001, and 0.1m respectively. The photosynthetic active radiation (PAR) was measured using PAR sensor (Chelsea Technologies, UK). Nutrients samples were collected in 100 ml plastic bottles, pigment samples were collected in 10L black plastic bottles and primary production (both total and size-fractionated) incubation samples were collected in 5L plastic bottles and subsampled to 1 L Nalgene plastic bottles.

2.2 Hydrographic measurements

The concentration of nutrients (nitrate, phosphate and silicate) were measured onboard, within one hour after sampling, using EcoLab autoanalyzer following the methods given in Grasshoff et al. (1983). The autoanalyzer is calibrated with the certified reference materials (CRMs) supplied by the Dr. M. Aoyama. We had prepared the working standards, which were calibrated with CRM and they are used for every profile. The detection limits for nitrate+nitrite, phosphate and silicate were 0.02, 0.02, and 0.02 µM respectively. About 10 L of water was filtered through GF/F (0.7 µm pore size; Whatman) in the dark and pigments retained on the filters were frozen in the liquid nitrogen until analysis. The pigments retained on the filters were first extracted to 90% acetone and measured using High Pressure Liquid Chromatography (HPLC) following Roy et al. (2015). SPM in the water is estimated by filtering ~5 litres of water through pre-weighted 0.22 µm polycarbonate filter

(Millepore) and dried at 50°C for over night (12 h). The weight of the SPM retained on the filter was measured by subtracting weight of the filter before filtration from that of after filtration. About 5 litres of the sample was filtered through pre-combusted (at 450° C for 6 hours) GF/F filters and dried at 50° C for 12 h. These filters were exposed to the concentrated hydrochloric acid for 12 hours to remove inorganic carbon on the filter. The content and atomic ratios of carbon of particulate organic matter (POM) retained on the filter was determined using Elemental analyser connected to Isotope Ratio Mass Spectrometer (IRMS; M/s. Elementar Analysensysteme, GmbH, Germany).

2.3. In vitro total primary production measurements

The total primary production, defined as all size classes of phytoplankton, in seawater at different light depths in the photic zone was measured using enriched sodium bicarbonate ($\text{NaH}^{13}\text{CO}_3$; 99%; Sigma Aldrich, USA) tracer following procedures given by Hama et al. (1983). Briefly, 1 L of seawater sample was taken from depths, where 100%, 90%, 75%, 50%, 25% and 1% of surface PAR reaches, into Nalgene transparent bottles and 0.2 mL of 2 mM enriched sodium bicarbonate spike was added and incubated in triplicate light and dark bottles in the deck incubator. The temperature in the incubator was maintained with running water from sea surface. Different light screens were used to cut the light for the deeper samples. One set of sample filtered immediately on pre-combusted GF/F filter and sample retained on filter was stored at -20° C until analysis for initial concentration of particulate organic carbon (POC) and atomic ratio of $^{13}/^{12}\text{C}$ measurements. Samples were incubated for 12 h (from dawn to dusk) and filtered through pre-combusted GF/F filters, dried at 50° C and exposed to the HCl fumes to remove inorganic carbon. In the onshore-based laboratory, the entire filter was packed in tin cups and introduced to Elemental analyser (Pyrocube; Elementar Analysensysteme, GmbH, Germany) coupled to a mass spectrometer (Isoprime 100, UK) to determine content and atomic ratios ($^{13}/^{12}\text{C}$) of particulate organic carbon.

About 1 L of sea water samples from different light depths were filtered through 10 μm , 2 μm and 0.2 μm filters (Millepore) and 0.2 ml of 2 mM of enriched sodium bicarbonate spike was added and incubated in triplicate in light and dark bottles for 12 h (dawn to dusk). As mentioned above for total primary production experiments, samples were filtered through pre-combusted GF/F filter, after incubation, and stored at -20C until analysis in the shore-based laboratory. The filters were treated in the same manner of total primary productivity measurement for measurement of organic carbon content and atomic ratios of carbon retained on the filter using elemental analyzer coupled to IRMS. Primary production (both total and size-fractionated) is computed from concentration of POC and atomic ratio of $^{13}\text{C}/^{12}\text{C}$ using the methodology given by Hama et al. (1983). The precision of the primary production measurement in terms of the CV was 5%.

2.4. Impact of cloud cover (light) on primary production

The surface water from different stations was collected in six 1L Nalgene bottles and was spiked with $^{13}\text{C}_{\text{NaHCO}_3}$. Three bottles were kept in the deck incubator at the natural light whereas the other 3 bottles were kept at high light ($981 \mu\text{mole photon m}^{-2}\text{s}^{-1}$) for 12 hours. After incubation time, samples were processed, as described in section 2.3, to examine the impact of light on primary production.

2.5. Computations

The mixed layer depth (MLD) was determined following Shankar et al. (2015) by estimating density at *in situ* temperature, salinity and pressure and subtracting $0.5 \text{ }^\circ\text{C}$ from temperature profile and estimated against density. The depth of MLD is taken where the difference in density at *in situ* temperature and $0.5 \text{ }^\circ\text{C}$ becomes zero. In this manner, the influence of changes in temperature and salinity on MLD is accounted (Shankar et al., 2015). The depth of nitracline was computed as the depth where the concentration of nitrate is $1 \mu\text{M}$. The photic zone depth was computed as the depth where 1% of surface light is observed. The statistical analysis was carried out using STATISTICA software and graphical representation was done using Ocean Data View (3-D plots) and Grapher (2-D plots).

3. Results

3.1 Hydrographic characteristics of the study region

Two CE and one ACEs were sampled during this study and all these eddies formed in the east or northeastern BoB (Fig. 1). The ACE was formed about 6 months before it was sampled whereas CE_N and CE_S were formed 3 and 2 months before they were sampled (Fig. 1). The vertical temperature structure indicates that the upper 60 m of water column is warm and highly mixed in the entire study region (Fig. 2a). Relatively cooler water was observed between 900 and 2000 kms of distance (stations 7 to 12) associating with high winds (>30 knots) caused by local depression (Figure is not shown). Decrease in temperature was observed below 60 m in CE and NE regions, in contrast, the entire 100 m of water column was warm in the ACE region (stns 4 to 7 and 17 to 18) (Fig. 2a). Upsloping of cooler waters were observed associated with CE (CE_N and CE_S). Similar to temperature, salinity was lower by 1 psu in the upper 60 m of water column compared to depth below in the CE, but the entire water column was filled with low salinity (~ 33.5) in the upper 100 m in the ACE region (Fig. 2b). Relatively low saline (<32) waters were observed in the northern BoB (stns. 11 to 13) compared to south (Fig. 2b). Increase in salinity was observed at stations between 14 and 15 associated with CE_S (Fig. 2b). The depth of mixed layer varied between 22 and 66m and deeper mixing was observed in the ACE and shallower in the CE regions (Fig. 2a). The depth of 28°C

isotherm was at 50 m depth under the CE, where sea surface level anomaly (SLA) was -0.2 m, and it was deepened to 90 to >100 m under the ACE region (Fig. 2a) associating with high SLA of >0.3m (Fig. 1). Similarly, the depth of 34 psu isohaline was at 40 m and it was deepened to 90->100 m under ACE and followed the 28 °C isotherm.

The photosynthetic active radiation (PAR) at surface varied between 82 and 850 $\mu\text{mol photons m}^{-2}\text{d}^{-1}$ in the entire cruise track and the least PAR was observed at stations 4 to 8 and the highest PAR was noticed between station 1-3 (Fig. 2c). The depth of photic zone (depth of 1% of surface PAR) was ranged between 48 and 68m and it was shallow in the northern Bay (Stations 10-12) associated with high SPM. The concentration of SPM varied between 3.2 and 31.2 mg l^{-1} and higher concentration of SPM (>20 mg l^{-1}) was observed in the northern (stations 8 to 12) compared to southern Bay (Fig. 2d). The inverse relation was observed between photic zone integrated SPM and photic depth (Fig. 3; $r^2=0.55$; $p<0.001$).

The concentration of nitrate was low (<0.5 μM) in the upper 80m of water column in the ACE region and up to 30 m in the NE region (Fig. 4a). Higher nitrate (>0.5 μM) concentrations were observed in the CE_S and CE_N than ACE region (Fig. 4a). Deepening of low nitrate contours to depth of 80 m was observed in the ACE region (Fig. 4a). Concentration of phosphate was low (<0.1 μM) in the upper 40 m of water column with low in the ACE and high in the CE regions (Fig. 4b). Dissolved inorganic silicate was low (<2 μM) in the upper 30 m of water column along the entire transect and increased with depth. No significant increase in silicate concentration was observed in CE region (Fig. 4c).

3.2. Spatial variations in phytoplankton pigments and size-fractionated biomass

Low concentration of Chl-a was observed between surface and 30 m of water column with prominent deep Chl-a maxima (DCM) between 40 and 90m depths (Fig. 5a). The concentration of Chl-a in DCM varied between 0.3 and 0.9 mg m^{-3} with large spatial variability associating with mixing. Surfacing of DCM was observed between 1000 and 1300 kms distance (Stn 8 and 9) associated shallowing of mixed layer depth (Fig. 2c). Increase in Chl-a was observed in the upper 50 m of water column in the ACE associated with convergence. Slight increase in Chl-a was observed in the CE region associating with increase in nutrients (Fig. 5a). The concentration of fucoxanthin (marker pigment for diatoms) was high in the DCM region and surfacing of the same was noticed at stations 8-9 associating with high Chl-a (Fig. 5b). The concentration of zeaxanthin (marker pigment for cyanobacteria) was high in the upper 50 m and decreased with depth (Fig. 5c). Low concentration of zeaxanthin was observed at stations 8, 9 and CE_N and CE_S region. The contribution of micro- and nanophytoplankton biomass to the total phytoplankton biomass was low 10-40% with higher

contribution in the DCM than surface waters (Fig. 5d,e). The picophytoplankton contributed significantly (40-80%) to the total phytoplankton biomass in the entire study region with dominant contribution in the CE than ACE region (Fig. 5f).

3.2. Spatial variation in total primary production in the BoB

The total primary productivity in the surface waters varied between 3.6 and 14.5 mgC m⁻³ d⁻¹ in the study region. Higher surface production (4.6-10.3 mgC m⁻³ d⁻¹) was noticed in the CE region than ACE region (Fig. 6a). The high total primary production (10-14.5 mgC m⁻³ d⁻¹) was observed with high Chl-a in the upper 10 m of water column and decreased with depth with no subsurface maxima. Photic zone integrated total primary production varied between 190 and 390 mgC m⁻²d⁻¹ in the Bay with high production in the CE (323±29mgC m⁻²d⁻¹) than ACE (224±27mgC m⁻²d⁻¹) and NE (260±37mgC m⁻²d⁻¹) regions (Table 2). Photic zone integrated primary production displayed linear relation with photic zone integrated Chl-a ($r^2=0.78$; $p<0.001$; Fig. 7a), nitrate ($r^2=0.80$; $p<0.001$; Fig. 7b), and phosphate ($r^2=0.85$; $p<0.001$; Fig. 7c) and inverse relationship with depth of euphotic depth ($r^2=0.48$; $p<0.001$; Fig. 7d), mixed layer ($r^2=0.62$; $p<0.001$; Fig 7e) and nitracline depth ($r^2=0.48$; $p<0.001$; Fig. 7f; Table 3).

3.3. Spatial variation in size-fractionated primary production in the BoB

The primary productivity by microphytoplankton in the surface waters varied between 1.3 and 13.8 mgC m⁻³ d⁻¹ in the study region with relatively higher in the CE (5.5±4 mgC m⁻³ d⁻¹) than ACE (2.7±2 mgC m⁻³ d⁻¹) followed by pico and nanophytoplanktons (Fig. 6b-d). The depth integrated primary production by microplankton was higher in the CE (164±16mgC m⁻²d⁻¹) than ACE (60±26mgC m⁻²d⁻¹) and NE (140±32mgC m⁻²d⁻¹) associating with higher nutrient concentrations in the photic zone (Table 2). The higher picophytoplankton primary production was observed in ACE (140±20 mgC m⁻²d⁻¹) followed by microplankton (60±26mgC m⁻²d⁻¹) and nanoplankton (28±19mgC m⁻²d⁻¹) associating with lower nutrients concentrations (Table 1,2). The photic zone integrated nutrients (nitrate and phosphate) displayed linear relation with photic zone integrated microphytoplankton production ($r^2=0.58$ and 0.49 with nitrate and phosphate respectively; Table 3) and inverse relation with photic zone integrated picophytoplankton production ($r^2=0.48$ and 0.37 respectively; Table 3). The nanophytoplankton production did not display significant relation with nutrients.

3.4. Impact of cloud cover (light) on primary production

The nitrate and phosphate concentrations of the surface water incubated at natural and artificial light varied between 0.02 to 1.6 µM and 0.04 to 0.22 µM respectively (Fig. 8a,b). Lower concentration of

nitrate was observed at stations 7 and 8 ($<0.1\mu\text{M}$) whereas it was above limiting levels at other stations. Similarly, phosphate was low at station 7 ($<0.05\mu\text{M}$) and it was above $0.05\mu\text{M}$ in other stations incubated. The *in situ* PAR varied from 120 to $818\mu\text{mol photon m}^{-2}\text{s}^{-1}$, and artificial light was kept at constant PAR of $891\mu\text{mol photon m}^{-2}\text{s}^{-1}$ (Fig. 8c). Insignificant variations in surface primary production was observed for samples incubated at natural light and artificial light at all stations (Fig. 8d). Neither surface primary production nor column production showed significant relation with surface PAR or photic zone integrated PAR in the study region (Figure not shown; $r^2=0.08$).

Discussion

4.1. Eddy-driven modifications in nutrients and pigments distribution in the BoB

The depth of both 28°C isotherm and 34 psu isohaline were found at shallow depth (40-50 m) under the CE whereas it was deepened to 90 to >100 m under ACE (Fig. 2a,b), associating with low (negative) SLA (-0.3 m) and high (positive) SLA (0.3 m) respectively (Fig. 1), suggesting occurrence of divergence and convergence respectively. Since eddies are formed in the BoB due to remote forcing through Rossby waves, the local wind impact is minimal (Chatterjee et al., 2017; Cheng et al., 2018). Mixed layer depth was shallow in the CE (35 ± 3 m) and deepened in the ACE (62 ± 4 m) further confirm the variable mixing within the CE and ACE (Fig. 2). High mixed layer mean concentrations of nutrients (1.26 ± 0.2 and $0.1\pm 0.01\mu\text{M}$ of nitrate and phosphate respectively; Fig. 4; Table 1) were observed in the CE region associated with divergence of high saline, cold and nutrient-rich waters from the depth below 50 to 100 m (Fig. 2). In contrast, the entire upper 100 m of water column is filled with low saline, warm and nutrient-poor waters (0.02 ± 0.01 and $0.04\pm 0.01\mu\text{M}$ of nitrate and phosphate respectively; Table 1) in the ACE region due to convergence of surface waters than NE region (0.43 ± 0.2 and $0.06\pm 0.01\mu\text{M}$ respectively; Table 1). Low nitrate concentrations in the ACE indicates possible role of nitrogen (N_2) fixers (Fig. 4a). ACEs are reported to be regions of N_2 fixation in the Pacific and Atlantic Oceans due to lack of dissolved inorganic nitrogen and warm water column (Fong et al., 2008; Loscher et al., 2016). Perennial occurrence of N_2 fixers, such as *Trichodesmium sp.*, were reported in the BoB during spring intermonsoon (Jyothibabu et al., 2006; Shetye et al., 2013), postmonsoon (Hedge et al., 2008) and summer monsoon (Paul et al., 2007; Wu et al., 2019) in the BoB indicating possible occurrence of N_2 fixation. Based on observed high $\delta^{15}\text{N}$ values of suspended particulate matter (6 and 9‰; Sherin et al., 2018; Sarma et al., 2019a), the occurrence of N_2 fixation can be ruled out in the BoB. Recently, Loscher et al. (2020) reported absence of N_2 fixation and it is attributed to limitation of micronutrients, other than iron, in the

BoB. Recently Sarma et al. (2019b) found that dissolved organic nitrogen (DON) supports primary production in the BoB in the absence of inorganic nitrogen. The concentration of DON in the BoB is reported to be ranged between 3 to 10 μM and they are an order of magnitude higher than inorganic nitrogen. Therefore, nitrogen may not be severely limiting primary production in the BoB.

Slight increase in Chl-a concentrations was observed in the ACE (stations 4-7) and part of NE (stations 8-9) due to mixing caused by convergence and high local winds (wind speed >10 m/s; Figure not shown) respectively as evidenced from surfacing of fucoxanthin from the depth of DCM (Fig. 5b). The higher depth integrated fucoxanthin was observed in CE ($2.0 \pm 0.3 \mu\text{g m}^{-2}$) than NE ($1.6 \pm 0.5 \mu\text{g m}^{-2}$) and ACE ($1.2 \pm 0.8 \mu\text{g m}^{-2}$; Table 1), in contrast, higher zeaxanthin was observed in ACE ($4.0 \pm 0.9 \mu\text{g m}^{-2}$) than CE ($2.8 \pm 0.5 \mu\text{g m}^{-2}$) and NE ($2.2 \pm 0.5 \mu\text{g m}^{-2}$) suggesting that dominant microphytoplankton in the CE and picophytoplankton in the ACE. The distribution of size-fractionated phytoplankton biomass is not uniform within the ACE as the fraction of nanophytoplankton biomass was higher (20-35%) in the eastern part of ACE (stations 4-7) than western region (10-15%; stations 17-18) (Fig. 5d-f). Similarly, higher picophytoplankton biomass contribution was observed in the western (70-80%) than eastern ACE (50-55%) due to variable mixing within the ACE as evidenced from deeper mixed layer in the latter (60-68 m) than former region (50-55 m) (Fig. 5d-f). The mean concentrations of nitrate in the photic zone were higher in the CE ($1.26 \pm 0.2 \mu\text{M}$) than NE ($0.43 \pm 0.2 \mu\text{M}$) and ACE regions ($0.02 \pm 0.01 \mu\text{M}$; Table 1). Similarly, the photic zone integrated Chl-a was also higher in the CE ($23.3 \pm 5 \text{ mg m}^{-2}$) than in the NE ($18.6 \pm 8 \text{ mg m}^{-2}$) than ACE ($14.2 \pm 3 \text{ mg m}^{-2}$) region and it is consistent with the low nutrients in the ACE region (Table 1). The photic zone integrated Chl-a displayed linear (positive) relation with photic zone integrated nitrate ($r^2=0.78$; $p<0.001$), and phosphate ($r^2=0.85$; $p<0.001$) (Fig. 7; Table 3) and insignificant relation was noticed with silicate indicating that dominant control of nitrate and phosphate on phytoplankton biomass over silicate.

4.2. Impact of eddies on total and size-fractionated primary production

The primary production was high at surface and decreased with depth with slight increase in subsurface between 25 and 50m depth is associated with subsurface Chl-a maxima in the study region (Fig. 5a). The photic zone integrated primary production was significantly higher in the CE ($323 \pm 29 \text{ mgC m}^{-2} \text{ d}^{-1}$) than ACE ($224 \pm 27 \text{ mgC m}^{-2} \text{ d}^{-1}$) and NE ($260 \pm 37 \text{ mgC m}^{-2} \text{ d}^{-1}$) ($t_{\text{stat}}=3.76$; $p<0.001$; Table 2). This study suggested that low (high) primary production occurs in the ACE (CE) due to convergence (divergence) of waters leading to depletion (repletion) of nutrients in the mixed layer (Kumar et al., 2007; Sarma et al., 2016; 2018). Kumar et al. (2004; 2007) reported 100%

increase in primary production in the CE region ($221 \text{ mgC m}^{-2} \text{ d}^{-1}$) compared to outside ($107 \text{ mgC m}^{-2} \text{ d}^{-1}$) in the BoB whereas the increase was only 20-40% in the present study. The difference in response of primary production within and outside eddy is caused by intensity of mixing and amount of nutrients brought to the photic zone by CE. It is further noticed that enhanced microphytoplankton production was observed in the CE ($164 \pm 16 \text{ mgC m}^{-2} \text{ d}^{-1}$) than ACE ($60 \pm 26 \text{ mgC m}^{-2} \text{ d}^{-1}$; Table 2) suggesting that increase in nitrate and phosphate due to upwelling supported microplankton production as significant amount of silicate is available in the mixed layer (Fig. 2). Since diatoms require more nitrate and phosphate than cyanobacteria (Lovstad and Bjondalen, 1990; Balode et al., 1998), the conducive conditions occurs for diatoms to grow in the CE, associating with high nitrate and phosphate concentrations, as evidenced from higher fucoxanthin (marker pigment for diatoms) than in the ACE. In contrast, the primary production by picophytoplankton was high in the ACE ($148 \pm 20 \text{ mgC m}^{-2} \text{ d}^{-1}$) than CE ($105 \pm 12 \text{ mgC m}^{-2} \text{ d}^{-1}$; Table 2) suggesting that low concentrations of nitrate and phosphate are sufficient for picophytoplankton production in ACE. Increase in *f*-ratio in the mixed layer within the CE (0.31) than ACE (0.19) was reported in the BoB and attributed to increase in nutrients inputs to the photic zone in the former region (Sherin et al., 2018; Sarma et al., 2019a). Vidya and Kumar (2013) found that 43% of increase in biogenic sinking carbon flux to deep waters is observed under the influence of CE than NE regions in the BoB. Sarma et al. (2018) noticed existence of intense oxygen minimum zone below the CE and attributed to enhanced sinking carbon fluxes. Ittekkot et al. (1991) found higher sinking carbon fluxes to the deep BoB, than even highly productive Arabian Sea, and attributed to ballast of organic matter in association with mineral particles. Though such impact is visible in the northern BoB, where high SPM is noticed (Ittekkot et al., 1991), on the other hand, high sinking carbon fluxes in the southern BoB is found to be sourced from *in situ* processes (Unger et al., 2006). This study, therefore, suggests that CEs enhance not only primary production but also the contribution by microphytoplankton production leading to increase in sinking carbon fluxes to the deep BoB.

Photic zone integrated primary production displayed linear relation with photic zone integrated Chl-*a* ($r^2=0.78$; $p<0.001$; Fig. 7a), nitrate ($r^2=0.80$; $p<0.001$; Fig. 7b), and phosphate ($r^2=0.85$; $p<0.001$; Fig. 7c) and inverse relationship with depth of euphotic depth ($r^2=0.48$; $p<0.001$; Fig. 7d), mixed layer ($r^2=0.62$; $p<0.001$; Fig 7e) and nitracline depth ($r^2=0.48$; $p<0.001$; Fig. 7f) suggest that nutrients brought by vertical mixing in the CE enhanced primary production in the BoB. Similarly, photic-zone integrated microphytoplankton production showed linear relationship with photic zone integrated nitrate ($r^2=0.58$; $p<0.001$) and phosphate ($r^2=0.49$; $p<0.001$) whereas picophytoplankton production showed inverse relation with nitrate ($r^2=0.48$; $p<0.001$) and phosphate ($r^2=0.37$; $p<0.05$)

indicating that low nutrients concentrations in the ACEs supported picophytoplankton production and vice versa for microphytoplankton production (Table 3). This study suggests that mixing in the upper ocean associated with eddies played significant role on controlling total and size fractionated primary production in the BoB.

4.3. Influence of PAR on primary production in the BoB

Surface production, at 100% PAR, ranged from 4.6 to 14.5 mgC m⁻³ d⁻¹ with relatively higher production in the CE region associated with higher nutrients than ACE region (4.5-9.9 mgC m⁻³ d⁻¹; Fig. 2c, 6a). The primary production (both total and size fractionated) showed maximum at surface and decreased with depth suggesting that absence of photoinhibition in the study region. Qasim (1982) reported absence of photoinhibition due to cloud cover in the BoB. The surface primary production showed weak inverse relation with surface PAR ($r^2=0.28$; $p<0.02$) whereas positive (linear) relation with surface Chl-a ($r^2=0.48$; $p<0.001$), nitrate ($r^2=0.47$; $p<0.001$), and phosphate ($r^2=0.50$; $p<0.001$) indicating that availability of nutrients are crucial for primary production than availability of light (Table 2).

Increased concentrations of SPM were observed in the northern Bay (Stations 10-12; Fig. 2d) compared to south leading to shallow photic depth in the former region. The inverse (negative) relationship was observed between depth of photic zone and photic depth integrated SPM indicating that SPM shallowed depth of photic zone at the rate of 0.02 m per 1 g m⁻² of SPM increased (Fig. 3). Though depth of photic zone was decreased in the northern Bay by 20 m (stations 10-12) due to high SPM (Fig. 3), the depth of photic zone showed inverse (negative) relation with photic zone integrated production (Fig. 7d) suggesting that decrease in photic depth in the northern Bay did not decrease photic zone production as major fraction of primary production occurred in the upper 25 m (Fig. 6a).

Jyothibabu et al. (2018) found that increase in Chl-a in the upper 40 m water column and decrease in depth below 40 m was observed associated with low underwater PAR and suggested that phytoplankton adopt to large changes in PAR. The ACE region was sampled twice with different light conditions. For instance, eastern part of ACE was sampled (stations 4 to 7), when underwater PAR at surface was 50-60 $\mu\text{mole photons m}^{-2} \text{ s}^{-1}$ and western part of ACE was sampled (stations 17-18), when surface PAR was $>500 \mu\text{mole photons m}^{-2} \text{ s}^{-1}$ (Fig. 2c). Slight increase in Chl-a was observed in the upper 60m of water column in the eastern ACE associated with low PAR (stations 4 to 7) and low Chl-a in the western ACE region associated with high PAR ($>500 \mu\text{mole photons m}^{-2} \text{ s}^{-1}$). The higher Chl-a in the eastern ACE is associated with deeper mixed layer (60-68 m) than

western ACE (50-55m) due to variable mixing rates within the ACE. Therefore, the changes in vertical distribution of Chl-a within the ACE may be influenced by physical mixing than under water PAR in the BoB (Fig. 2c and 5a).

The total photosynthesis per unit Chl-a (P_B ; in $\text{mgC}(\text{Chl-a})^{-1} \text{d}^{-1}$) is ranged between 8.0 and 16.2 $\text{mgC}(\text{Chl-a})^{-1} \text{d}^{-1}$ in the study region and the mean P_B in the ACE ($14.1 \pm 1.5 \text{ mgC}(\text{Chl-a})^{-1} \text{d}^{-1}$) and CE ($11.0 \pm 3 \text{ mg}(\text{Chl-a})^{-1} \text{d}^{-1}$) are statistically insignificant. Waite et al. (2019) also noticed insignificant differences in P_B in the CE and ACE in the southwestern Indian Ocean. The mean P_B values observed in this study are significantly higher than Gomes et al. (2000) during peak southwest monsoon period (7.0 ± 1.4 and $5.6 \pm 4.0 \text{ mgC}(\text{Chl-a})^{-1} \text{d}^{-1}$ respectively in the inshore and offshore regions) but within the range found during non-monsoon seasons ($10\text{-}40 \text{ mgC}(\text{Chl-a})^{-1} \text{d}^{-1}$; Gomes et al., 2000). Such difference may probably be caused by variations in SPM concentration in the water column. Gomes et al. (2000) study was conducted close to coast during peak summer monsoon period when higher SPM concentrations were reported in the coastal waters (Sarma et al., 2012). Occurrence of coastal upwelling is reported along the east coast of India during summer resulting in enhanced nutrients and Chl-a in the inshore waters (Shetye et al., 1991; Sarma et al., 2013). Based on the SeaWiFS images, the offshore advection of upwelled water possibly increased phytoplankton biomass in the offshore region (Gomes et al., 2000). Though high Chl-a concentrations were observed by Gomes et al. (2000), however low P_B values were caused by increase in suspended matter. On the other hand, the P_B values for microphytoplankton was significantly higher in the microplankton (50 ± 8 , 42 ± 6 and $36 \pm 8 \text{ mg}(\text{Chl-a}) \text{d}^{-1}$) in ACE, CE and NE regions respectively) than nano (3 ± 1 , 5 ± 2 , $4 \pm 1 \text{ mg}(\text{Chl-a}) \text{d}^{-1}$ respectively) and picoplankton (11 ± 4 , 16 ± 5 , $11 \pm 3 \text{ mg}(\text{Chl-a}) \text{d}^{-1}$ respectively) suggesting that microplankton efficiently fix inorganic carbon than other size classes in the BoB. The mean P_B in the picoplankton and total phytoplankton were almost same as picoplankton contributed $>70\%$ to the total phytoplankton biomass. The variability in P_B in any size class is not significantly different within CE, ACE and NE regions.

It is further noticed that despite high PAR and nutrients is available during northeast (winter) monsoon, the primary production was almost equal to that of summer monsoon ($300 \text{ mgC m}^{-2} \text{d}^{-1}$ during both seasons; Gomes et al., 2000), clearly indicating that light is not controlling primary production in the BoB.

In order to further confirm the impacts of cloud cover or PAR on primary production, laboratory experiment was conducted for the surface samples collected from different stations at *in situ* (natural) and artificial light conditions. The nitrate and phosphate concentrations in the surface waters incubated varied from 0.04 to 1.6 μM and 0.04 to 0.23 μM respectively (Fig. 8a,b). The artificial

light in the incubation bottle was more than 10 to 60% from that of natural PAR (Fig. 8c). Despite increase in PAR, the changes in primary production was within the measurement errors (Fig. 8d). It is also possible that insignificant difference in PP under natural and artificial PAR may be caused by nutrient limitation. The Figure 8 suggests that despite increase in PAR by artificial light did not increase primary production in the entire study region strongly indicating that light is not limiting primary production in the BoB (Fig. 8). This experiment strongly suggested that primary production in the BoB is strongly controlled by availability of nutrients, but not light during study period.

5. Summary and Conclusions

In order to examine the spatial variability and limitation factors of primary production, 18 stations were occupied during summer monsoon (11-29 June 2019) in the BoB. The upper ocean was strongly stratified due to freshwater discharge from major rivers. Low nutrients concentrations were noticed in the ACE regions due to downwelling and contrasting conditions were observed in the CE region due to upwelling of subsurface waters. Prominent existence of deep Chl-a maximum (DCM) was found at the depth of 40 to 90 m in the study region and its depth seems to be controlled by mixing associated with either eddy (CE or ACE) or local winds. Dominant fucoxanthin (marker pigment for diatoms) concentration was found in the DCM and zeaxanthin in upper 50m of water column. The depth of photic zone showed inverse relation with SPM with shallow in the north. The high rate of primary production by microplankton was observed in the CE whereas picoplankton production in the ACE. The photic zone integrated primary production displayed linear relation with photic zone integrated nutrients (nitrate and phosphate) and Chl-a but inverse relation with photic depth, mixed layer depth and nitracline depth suggesting that nutrients availability due to mixing controls the primary production in the BoB than light. The photic zone integrated microplankton production showed linear relation with photic zone integrated nutrients (nitrate and phosphate) whereas inverse relation with picoplankton production suggesting that availability of nutrients by eddies modify primary production by different size classes. The primary production measurements under controlled and *in situ* light conditions suggest that light did not affect rate of primary production in the BoB. This study strongly suggests that eddies modify availability of nutrients in the photic zone resulting in variations in primary production by different size classes than hitherto hypothesized as light limitation in the BoB.

Acknowledgements:

We would like to thank Director and Scientist-In-Charge for their encouragement and support. We would like to thank Ministry of Earth Science for funding and ship time of ORV Sagar Nidhi. We

would like to than Director, INCOIS for sanction of project “Influence of eddies on oxygen minimum zone and carbon sequestration” under O-MASCOT. We also would like to appreciate the help tendered by Ship’s crew, and other participants of the cruise during collection of samples.

References

Anand, S., Rengarajan, R., Sarma, V. V. S. S., Sudheer, A. K., Bhushan, R., and Singh, S. K. 2017. Spatial variability of upper ocean POC export in the Bay of Bengal and the Indian Ocean determined using particle-reactive ^{234}Th . *J. Geophys. Res.: Oceans*, 122, 3753-3770.

Balode, M., Purina, I., Bechemin, C., and Maestrini, S. 1998. Effects of nutrient enrichment on the growth rates and community structure of summer phytoplankton from the Gulf of Riga, Baltic Sea. *J. Plankt. Res.*, 20, 2251-2272.

Chatterjee, A., Shankar, D, McCreary, J.P., Vinayachandran, P.N., and Mukherjee, A. 2017. Dynamics of Andaman Sea circulation and its role in connecting the equatorial Indian Ocean to the Bay of Bengal. *J. Geophys. Res.*, 122, 1-19.

Chen, G., Wang, D. and Hou, Y. 2012. The features and interannual variability mechanism of mesoscale eddies in the Bay of Bengal. *Cont. Shelf Res.*, 47, 178-185.

Cheng, X., Xie, S.P., McCreary, J.P., Qi, Y., and Du, Y. 2013. Intraseasonal variability of sea surface height over the Bay of Bengal. *J. Geophys. Res.*, 118, 1-15.

Cheng, X., McCreary, J.P., Qiu, B., Qi, Y., Du, Y., and Chen, X. 2018. Dynamics of Eddy Generation in the Central Bay of Bengal. *J. Geophys. Res.*, 123, 8681-6875.

Fong, A.A., Karl, D.M., Lukas, R., Letelier, R.M., Zehr, J.P. and Church, M.J., 2008. Nitrogen fixation in an anticyclonic eddy in the oligotrophic North Pacific Ocean. *The ISME journal*, 2, 663-676

Grasshoff, K., Ehrhardt, M., Kremling, K. (Eds.), 1983. *Methods of Seawater Analysis*. Verlag Chemie, Weinheim.

Gomes, H.R., Goes, J.I. and Saino, T., 2000. Influence of physical processes and freshwater discharge on the seasonality of phytoplankton regime in the Bay of Bengal. *Cont. Shelf Res.*, 20, 313-330.

Gauns, M., Madhupratap, M., Ramaiah, N., Jyothibabu, R., Fernandes, V., Paul, J.T. and Kumar, S.P., 2005. Comparative accounts of biological productivity characteristics and estimates of carbon fluxes in the Arabian Sea and the Bay of Bengal. *Deep Sea Res. Part II: Topical Studies in Oceanography*, 52, 2003-2017.

Hama, T., Miyazaki, T., Ogawa, Y., Iwakuma, T., Takahashi, M., Otsuki, A. and Ichimura, S., 1983. Measurement of photosynthetic production of a marine phytoplankton population using a stable ^{13}C isotope. *Mar. Biol.*, 73,31-36.

- Hedge, S., Anil, A.C., Patil, J.S., Mitbavkar, S., Venkat, K., Gopalakrishna, V.V., 2008. Influence of environmental settings on the prevalence of *Trichodesmium* spp. in the Bay of Bengal. *Mar. Ecol. Prog. Ser.*, 356, 93–101.
- Hoglander, H., Larsson, U., and Hajdu, S. 2004. Vertical distribution and settling of spring phytoplankton in the offshore NW Baltic Sea proper. *Mar. Ecol. Prog. Ser.* 283, 15-27.
- Ittekkot, V., Nair, R.R., Honjo, S., Ramaswamy, V., Bartsch, M., Manganini, S. and Desai, B.N., 1991. Enhanced particle fluxes in Bay of Bengal induced by injection of fresh water. *Nature*, 351, 385-388.
- Jyothibabu, R., Madhu, N.V., Maheswaran, P.A., Asha Devi, C.R., Balasubramanian, T., Nair, K.K.C., Achuthankutty, C.T. 2006. Environmentally-related seasonal variation in symbiotic associations of heterotrophic dinoflagellates with cyanobacteria in the western Bay of Bengal. *Symbiosis*, 42, 51-58.
- Jyothibabu, R., Madhu, N.V., Maheswaran, P.A., Jayalakshmy, K.V., Nair, K.K.C. and Achuthankutty, C.T., 2008. Seasonal variation of microzooplankton (20–200 μm) and its possible implications on the vertical carbon flux in the western Bay of Bengal. *Cont. Shelf Res.*, 28, 737-755.
- Jyothibabu, R., Arunpandi, N., Jagadeesan, L., Karnan, C., Lallu, K.R. and Vinayachandran, P.N., 2018. Response of phytoplankton to heavy cloud cover and turbidity in the northern Bay of Bengal. *Sci.Rep.*, 8, 11282.
- Krishna, M.S., Prasad, V.R., Sarma, V.V.S.S., Reddy, N.P.C., Hemalatha, K.P.J. and Rao, Y.V., 2015. Fluxes of dissolved organic carbon and nitrogen to the northern Indian Ocean from the Indian monsoonal rivers. *J. Geophys. Res.: Biogeosci.*, 120, 2067-2080.
- Kumar S.P., Muraleedharan, P.M., Prasad, T.G., Gauns, M., Ramaiah, N., De Souza, S.N., Sardesai, S. and Madhupratap, M., 2002. Why is the Bay of Bengal less productive during summer monsoon compared to the Arabian Sea?. *Geophys. Res. Lettrs*, 29, 88-91.
- Kumar, S.P., Nuncio, M., Ramaiah, N., Sardesai, S., Narvekar, J., Fernandes, V. and Paul, J.T., 2007. Eddy-mediated biological productivity in the Bay of Bengal during fall and spring intermonsoons. *Deep Sea Res. Part I: Oceanographic Research Papers*, 54, 1619-1640.
- Kumar, S.P., Narvekar, J., Nuncio, M., Kumar, A., Ramaiah, N., Sardesai, S., Gauns, M., Fernandes, V. and Paul, J., 2010. Is the biological productivity in the Bay of Bengal light limited?. *Curr.Sci.*, 1331-1339.
- Löscher, C.R., Bourbonnais, A., Dekaezemacker, J., Charoenpong, C.N., Altabet, M.A., Bange, H.W., Czeschel, R., Hoffmann, C. and Schmitz, R., 2016. N₂ fixation in eddies of the eastern tropical South Pacific Ocean. *Biogeosciences*, 13, 2889-2899.
- Loscher, C.R., Mohr, W., Bange, H.W., and Canfield, D.E. 2020. No nitrogen fixation in the Bay of Bengal. *Biogeosciences*, 17, 851-864.
- Lovstad, O.m and Bjorndalen, K. 1990. Nutrients (P,N,Si) and growth conditions for diatoms and *Oscillatoria* spp. in lakes of south-eastern Norway. *Hydrobiologia*, 196, 255-263.

Madhupratap, M., Gauns, M., Ramaiah, N., Kumar, S.P., Muraleedharan, P.M., De Sousa, S.N., Sardessai, S. and Muraleedharan, U., 2003. Biogeochemistry of the Bay of Bengal: physical, chemical and primary productivity characteristics of the central and western Bay of Bengal during summer monsoon 2001. *Deep Sea Res., Part II: Topical Studies in Oceanography*, 50, 881-896.

Madhu, N.V., Jyothibabu, R., Maheswaran, P.A., Gerson, V.J., Gopalakrishnan, T.C. and Nair, K.K.C., 2006. Lack of seasonality in phytoplankton standing stock (chlorophyll a) and production in the western Bay of Bengal. *Cont. Shelf Res.*, 26, 1868-1883.

McDonnell, A. and Buesseler, K. 2012. A new method for the estimation of sinking particle fluxes from measurements of the particle size distribution, average sinking velocity, and carbon content. *Limnol. Oceanogr.: Methods*, 10, 329–346.

Milliman, J. D., and Meade, R. H. 1983. World-wide delivery of river sediment to the oceans, *J. Geol.*, 91, 1–21.

Milliman, J. D., and Syvitski, J. P. M. 1992. Geomorphic/tectonic control of sediment discharge to the ocean: The importance of small mountainous rivers, *J. Geol.*, 100, 525–544.

Mitchell, B.G., Brody, E.A., Holm-Hansen, O., McClain, C. and Bishop, J., 1991. Light limitation of phytoplankton biomass and macronutrient utilization in the Southern Ocean. *Limnol. Oceanogr.*, 36, 1662-1677

Mukherjee, A., Chatterjee, A., and Francis, P.A. 2019. Role of Andaman and Nicobar Islands in eddy formation along western boundary of the Bay of Bengal. *Sci. Rep.*, 9, 10152, doi: 10.1038/s41598-019-46542-9.

Omand, M.M., Govindarajan, R., He, J., and Mahadevan, A. 2020. Sinking flux of particulate organic matter in the oceans: Sensitivity to particle characteristics. *Sci. Rep.*, 10: 5582, doi:10.1038/s41598-020-60424-5.

Paul, J.T., Ramaiah, N., Gauns, M. and Fernandes, V., 2007. Preponderance of a few diatom species among the highly diverse microphytoplankton assemblages in the Bay of Bengal. *Mar. Biol.*, 152, 63-75.

Paul, J.T., Ramaiah, N. and Sardessai, S., 2008. Nutrient regimes and their effect on distribution of phytoplankton in the Bay of Bengal. *Mar. Envir. Res.*, 66, 337-344.

Qasim, S.Z. 1977. Biological productivity of the Indian Ocean. *Indian J. Mar. Sci.*, 6, 122-137.

Qasim, S.Z., 1982. Oceanography of the northern Arabian Sea. *Deep Sea Res. Part A. Oceanographic Research Papers*, 29, 1041-1068.

Radhakrishna, K., Bhattathiri, P.M.A. and Devassy, V.P., 1978. Primary productivity of the Bay of Bengal during August-September 1976. *Indian J. Mar. Sci.*, 7, 94-98.

Roy, S., Sathyendranath, S. and Platt, T., 2017. Size-partitioned phytoplankton carbon and carbon-to-chlorophyll ratio from ocean colour by an absorption-based bio-optical algorithm. *Remote Sensing of Environ.*, 194, 177-189.

Sakshaug, E. and Holm-Hansen, O., 1986. Photoadaptation in Antarctic phytoplankton: variations in growth rate, chemical composition and P versus I curves. *J. Plankton Res.*, 8, 459-473.

Sarma, V.V.S.S., Krishna, M.S., Rao, V.D., Viswanadham, R., Kumar, N., Kumari, T.R., Gawade, L., Ghatkar, S., and Tari, A. 2012. Sources and sinks of CO₂ in the west coast of Bay of Bengal. *Tellus-B*, 64, 10961, doi: 10.3402/tellusb.v64i0.10961.

Sarma, V.V.S.S., Krishna, M.S., Viswanadham, R., Rao, G.D., Rao, V.D., Sridevi, B., Kumar, B.S.K., Prasad, V.R., Subbaiah, Ch.V., Acharyya, T., Bandopadhyay, D., 2013b. Intensified oxygen minimum zone on the western shelf of Bay of Bengal during summer monsoon: influence of river discharge. *J. Oceanogra.*, 69, 45–55.

Sarma, V.V.S.S., Krishna, M.S., Prasad, V.R., Kumar, B.S.R., Naidu, S.A., Rao, G.D., Viswanadham, R., Sridevi, T., Kumar, P.P., and Reddy, N.P.C. 2014. Distribution and sources of particulate organic matter in the Indian monsoonal estuaries during monsoon. *Journal of Geophysical research: Biogeosciences*, doi:10.1002/2014JG002721.

Sarma, V.V.S.S., Rao, G.D., Viswanadham, R., Sherin, C.K., Salisbury, J., Omand, M.M., Mahadevan, A., Murty, V.S.N., Shroyer, E.L., Baumgartner, M. and Stafford, K.M., 2016. Effects of freshwater stratification on nutrients, dissolved oxygen, and phytoplankton in the Bay of Bengal. *Oceanography*, 29, 222-231.

Sarma, V.V.S.S., Jagadeesan, L., Dalabehera, H.B., Rao, D.N., Kumar, G.S., Durgadevi, D.S., Yadav, K., Behera, S. and Priya, M.M.R., 2018. Role of eddies on intensity of oxygen minimum zone in the Bay of Bengal. *Cont. Shelf Res.*, 168, 48-53.

Sarma, V.V.S.S., Yadav, K. and Behera, S., 2019a. Role of eddies on organic matter production and f-ratios in the Bay of Bengal. *Mar. Chemistry*, 210, 13-23.

Sarma, V.V.S.S., Rao, D.N., Rajula, G.R., Dalabehera, H.B. and Yadav, K., 2019b. Organic nutrients support high primary production in the Bay of Bengal. *Geophys. Res. Lettrs.*, 46, 6706-6715.

Shankar, D., Remya, R., Vinayachandran, P.N., Chatterjee, A., Behera, A. 2015. Inhibition of mixed-layer deepening during winter in the northeastern Arabian Sea by the West India Coastal Current. *Clim. Dyn.*, 47, 1049-1072.

Sherin, C.K., Sarma, V.V.S.S., Rao, G.D., Viswanadham, R., Omand, M.M. and Murty, V.S.N., 2018. New to total primary production ratio (f-ratio) in the Bay of Bengal using isotopic composition of suspended particulate organic carbon and nitrogen. *Deep Sea Res. Part I: Oceanographic Research Papers*, 139, 43-54.

Shetye, S.R., Gouveia, A.D., Shenoi, S.S.C., Michael, G.S., Sundar, D., Almeida, A.M. and Santanam, K., 1991. The coastal current off western India during the northeast monsoon. *Deep Sea Res., Part I*, 38, 1517-1529.

Sheye, S., Sudhakar, M., Jena, B., and Mohan, R. 2013. Occurrence of Nitrogen fixing cyanobacterium *Trichodesmium* under Elevated pCO₂ conditions in the Western Bay of Bengal, *International J. Oceanogr.*, 8, 10.1155/2013/350465.

Suess, E. 1980. Particulate organic carbon flux in the oceans surface productivity and oxygen utilization. *Nature*, 288, 260–263.

Thompson, P.A., Pesant, S., and Waite, A.M. 2007. Contrasting the vertical differences in the phytoplankton biology of a dipole pair of eddies in the south-eastern Indian Ocean. *Deep-Sea Res. II*, 54, 1003-1028.

Vidya, P.J. and Kumar, S.P., 2013. Role of mesoscale eddies on the variability of biogenic flux in the northern and central Bay of Bengal. *J. Geophys. Res: Oceans*, 118, 5760-5771.

Unger, D., V. Ittekkot, P. Schafer, J. Tiemann, and S. Reschke (2003), Seasonality and interannual variability of particle fluxes to the deep Bay of Bengal: Influence of riverine input and oceanographic processes, *Deep Sea Res., Part II*, 50, 897–923.

Unger, D., Schafer, P., Ittekkot, V., and Gaye, B. 2006. Nitrogen isotopic composition of sinking particles from the southern Bay of Bengal: Evidence for variable nitrogen sources. *Deep-Sea Res.*, 53, 1658-1676.

Waga, H., Hirawake, T., and Ueno, H. 2019. Impacts of mesoscale eddies on phytoplankton size structure. *Geophys. Res. Lett.*, 46, doi: 10.1029/2019GL085150.

Waite, A.M., Blengang, P.K., and Harrison, P.J. 1992. Spring bloom sedimentation in a sub-arctic ecosystem: 1. Nutrient sensitivity. *Mar. Biol.*, 114, 119-129.

Waite, A.M., Pesant, S., Griffin, D.A., Thompson, P.A., and Holl, C.M. 2007. Oceanography, primary production and dissolved inorganic nitrogen uptake in two Leeuwin Current eddies. *Deep-Sea Res. II*, 54, 981-1002.

Waite, A.M., Raes, E., Beckley, L.E., Thompson, P.A., Griffin, D., Saunders, M., Sawstrom, C., O'Rourke, R., Wang, M., Landrum, J.P., and Jeffs, A. 2019. Production and ecosystem structure in cold-core vs. warm-core eddies: implications for the zooplankton isoscape and rock lobster larvae. *Limnol. Oceanogr.*, 64, 2405-2423.

Wu, C., Kan, J., Liu, H., Pujari, L., Guo, C., Wang, X., and Sun, J. 2019. Heterotrophic bacteria dominate the diazotrophic community in the eastern Indian Ocean during pre-southwest monsoon. *Microbial Ecol.*, 10.1007/s00248-019-01355-1.

Yun, M.S., Chung, K.H., Zimmermann, S., Zhao, J., Joo, H.M. and Lee, S.H., 2012. Phytoplankton productivity and its response to higher light levels in the Canada Basin. *Polar Biol.*, 35, 257-268.

Table 1: The photic zone mean concentrations of nutrients and photic zone integrated concentrations of pigments in the CE, ACE and NE regions.

Region	Temp (°C)	Salinity (psu)	NO ₃ (μM)	PO ₄ (μM)	SiO ₄ (μM)	Chl-a (mg m ⁻²)	Fuco (μg m ⁻²)	Zea (μg m ⁻²)
CE	30.01±0.1	33.68±0.02	1.26±0.2	0.10±0.01	1.9±0.8	23.3±5	2.0±0.3	3.0±0.9
ACE	30.29±0.1	33.50±0.02	0.02±0.01	0.04±0.01	1.8±0.6	14.2±3	1.2±0.8	4.0±0.9
NE	29.92±0.2	33.08±0.01	0.43±0.2	0.06±0.01	2.3±0.4	18.6±8	1.6±0.5	2.2±0.5

Table 2: The mean photic zone integrated total primary production, micro-, nano- and picophytoplankton production in the CE, ACE and NE regions.

Region	Total PP (mgC m ⁻² d ⁻¹)	Microplankton PP (mgC m ⁻² d ⁻¹)	Nanoplankton PP (mgC m ⁻² d ⁻¹)	Picoplankton PP (mgC m ⁻² d ⁻¹)
CE	323±29	164±16	38±28	105±12
ACE	224±27	60±26	28±19	148±8
NE	260±37	140±32	20±8	99±22

Table 3: Spearman correlation among different parameters in the study region

Relation	r ²	p-value
Photic depth vs photic zone integrated SPM	0.55	<0.001
Photic depth integrated Chl-a vs nitrate	0.78	<0.001
Photic depth integrated Chl-a vs phosphate	0.85	<0.001
Surface PAR vs Surface total primary production	0.28	<0.02
Surface total PP vs surface Chl-a	0.48	<0.001
Surface total PP vs surface nitrate	0.47	<0.001
Surface total PP vs surface phosphate	0.50	<0.001
Photic depth integrated total PP vs Chl-a	0.78	<0.001
Photic depth integrated total PP vs nitrate	0.80	<0.001
Photic depth integrated total PP vs phosphate	0.85	<0.001
Photic depth integrated total PP vs photic depth	0.48*	<0.001
Photic depth integrated total PP vs mixed layer depth	0.62*	<0.001
Photic depth integrated total PP vs nitracline depth	0.48	<0.001
Photic depth integrated microplankton PP vs nitrate	0.58	<0.001
Photic depth integrated microplankton PP vs phosphate	0.49	<0.001
Photic depth integrated picoplankton PP vs nitrate	0.48*	<0.001
Photic depth integrated picoplankton PP vs phosphate	0.37*	<0.05

* indicates inverse relation

Legend to Figures

Figure 1. The study region with station locations and identified station numbers. The color shading shows the Sea Level Anomaly (SLA) variations depicting the surface circulation and meso-scale cyclonic eddies (CE_N and CE_S) and anticyclonic eddy (ACE) in the Bay of Bengal. Vectors denote the direction and speed of the geostrophic currents at the surface. The magnitude of current vector is shown in the left-top corner. The track of each eddy is shown as a line and the date of origin and date of sampling. The Primary production experiments were conducted at stations marked with white closed circles.

Figure 2: Vertical distribution of (a) temperature ($^{\circ}C$), (b) Salinity, c) photosynthetic active radiation (PAR; $\mu\text{mol photons m}^{-2} \text{ s}^{-1}$), and d) Suspended Particulate Matter (SPM; mg l^{-1}) along the cruise track in the BoB. Station numbers and stations considered under CE_S , ACE, and CE_N regions are shown. The depth of photic zone (white line) and mixed layer depth (black line) are shown.

Figure 3: The relationship between depth of photic zone and concentration of SPM in the BoB.

Figure 4: Vertical distribution of (a) nitrate (μM), (b) phosphate (μM), and (c) Silicate (μM) in the color scale along the cruise track in the BoB. Station numbers and stations considered under CE_S , ACE and CE_N regions are shown.

Figure 5: Vertical distribution of a) Chlorophyll-a (mg m^{-3}), b) fucoxanthin ($\mu\text{g m}^{-3}$), c) zeaxanthin ($\mu\text{g m}^{-3}$), contribution of d) microplankton (%), e) nanoplankton (%) and f) picoplankton (%) to the total phytoplankton biomass. Station numbers and stations considered under CE_S , ACE and CE_N regions are shown.

Figure 6: Vertical distribution of (a) total primary production rates ($\text{mgC m}^{-3} \text{ d}^{-1}$), (b) microphytoplankton c) nanophytoplankton and d) picophytoplankton production. All production rates in $\text{mgC m}^{-3} \text{ d}^{-1}$. Station numbers and stations considered under CE_S , ACE and CE_N regions are shown.

Figure 7: Relationship of photic zone integrated primary production with a) Chl-a (mg m^{-2}), b) Nitrate (mM m^{-2}), c) phosphate (mM m^{-2}), d) euphotic depth (m), e) mixed layer depth (m), and f) nitracline depth (m) in the BoB.

Figure 8: The concentration of a) nitrate, b) phosphate, in the surface waters and primary production (red bars) incubated a) under surface PAR (natural light) and d) under artificial light (blue). Variation in triplicate incubation primary production are shown as error bars. The station numbers are also given on the upper axis.

Figure 1

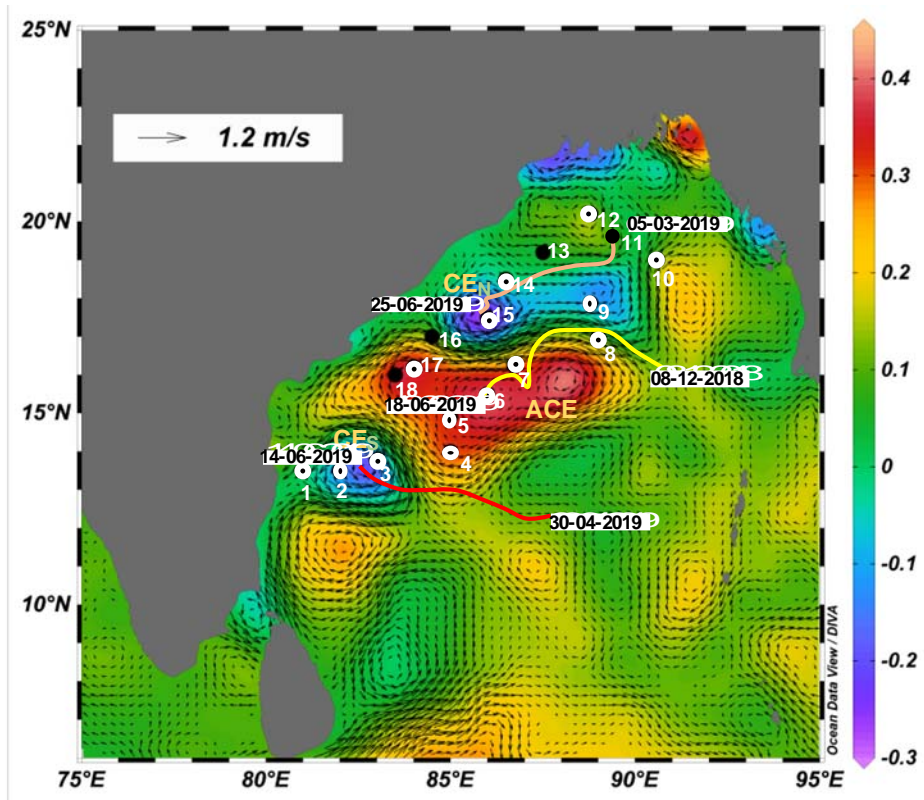


Figure 2

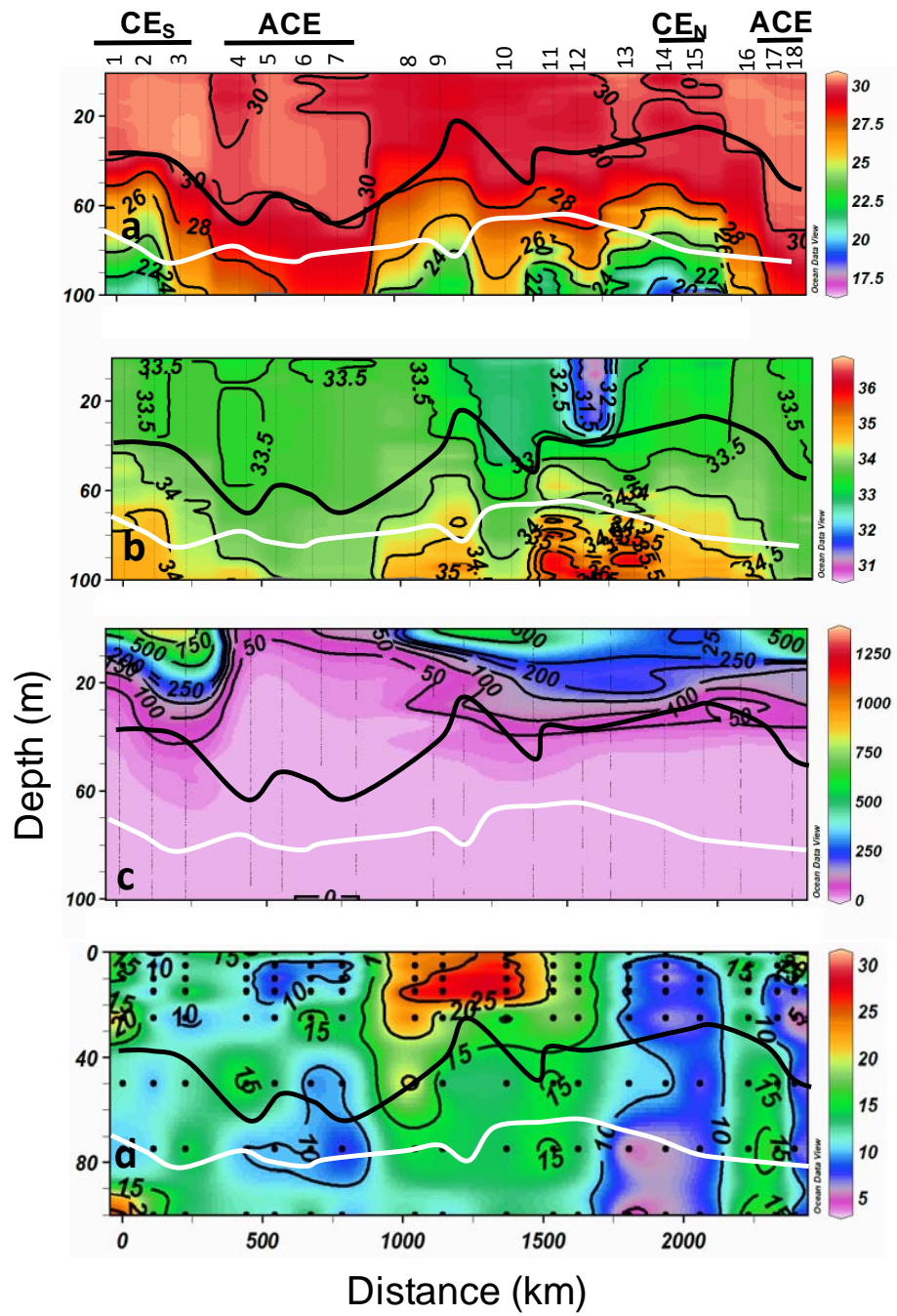


Figure 3

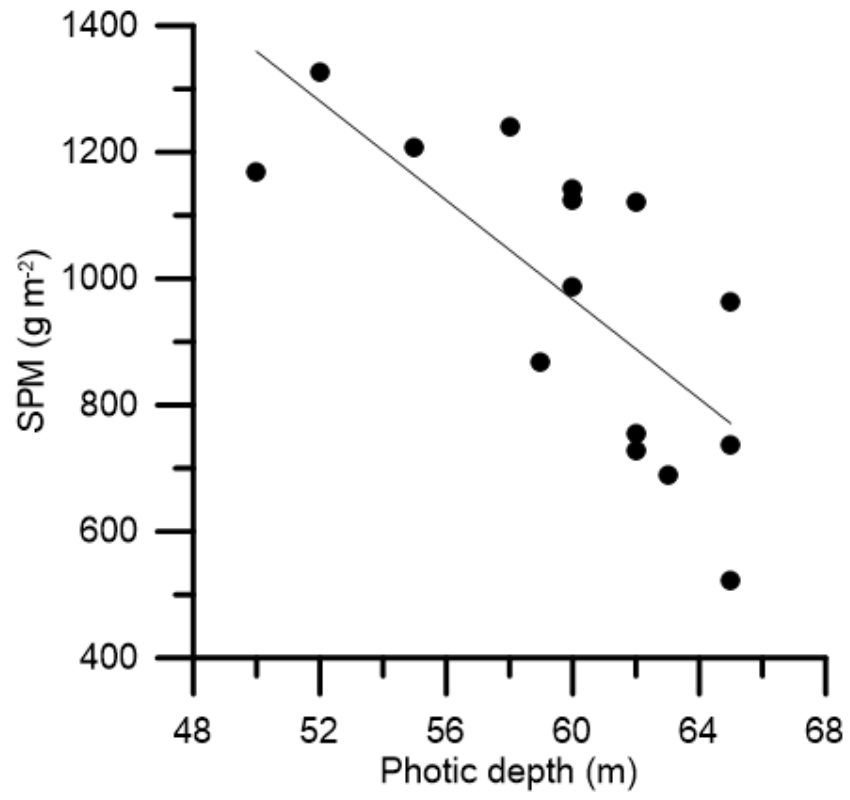


Figure 4

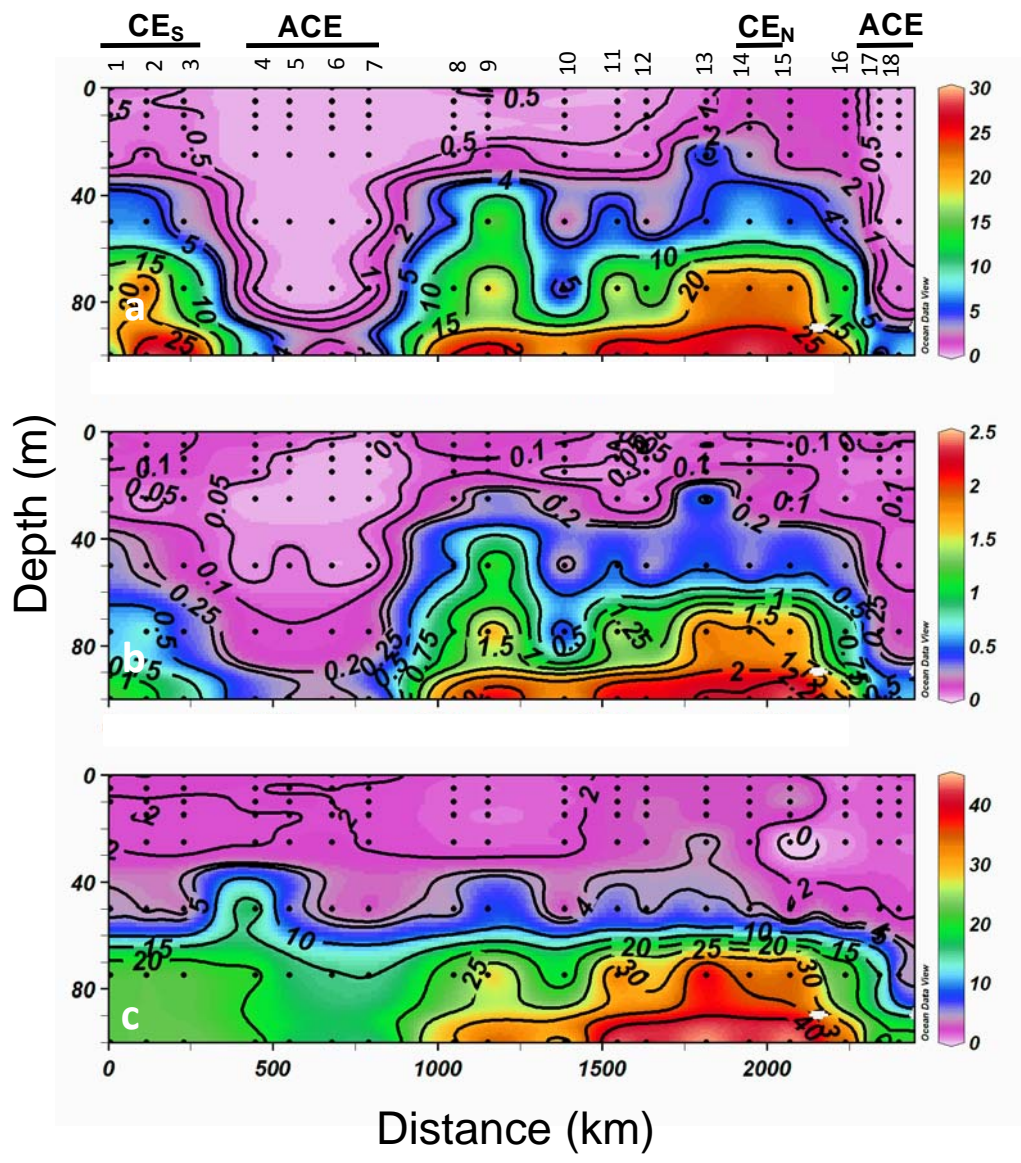


Figure 5

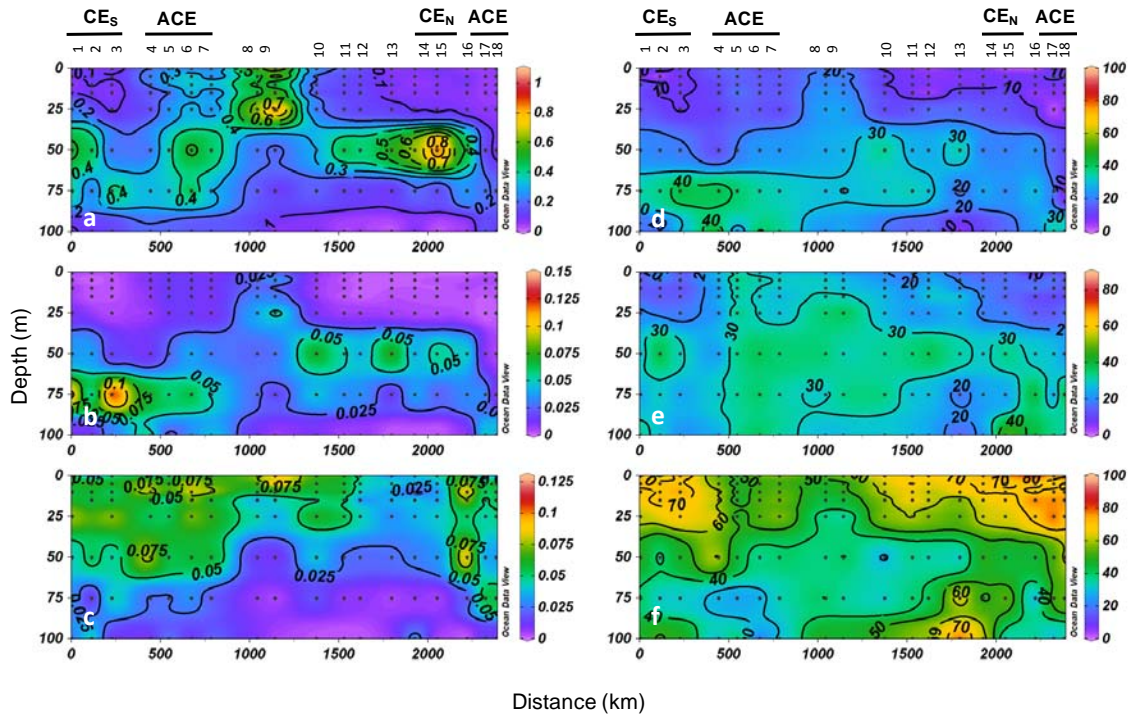


Figure 6

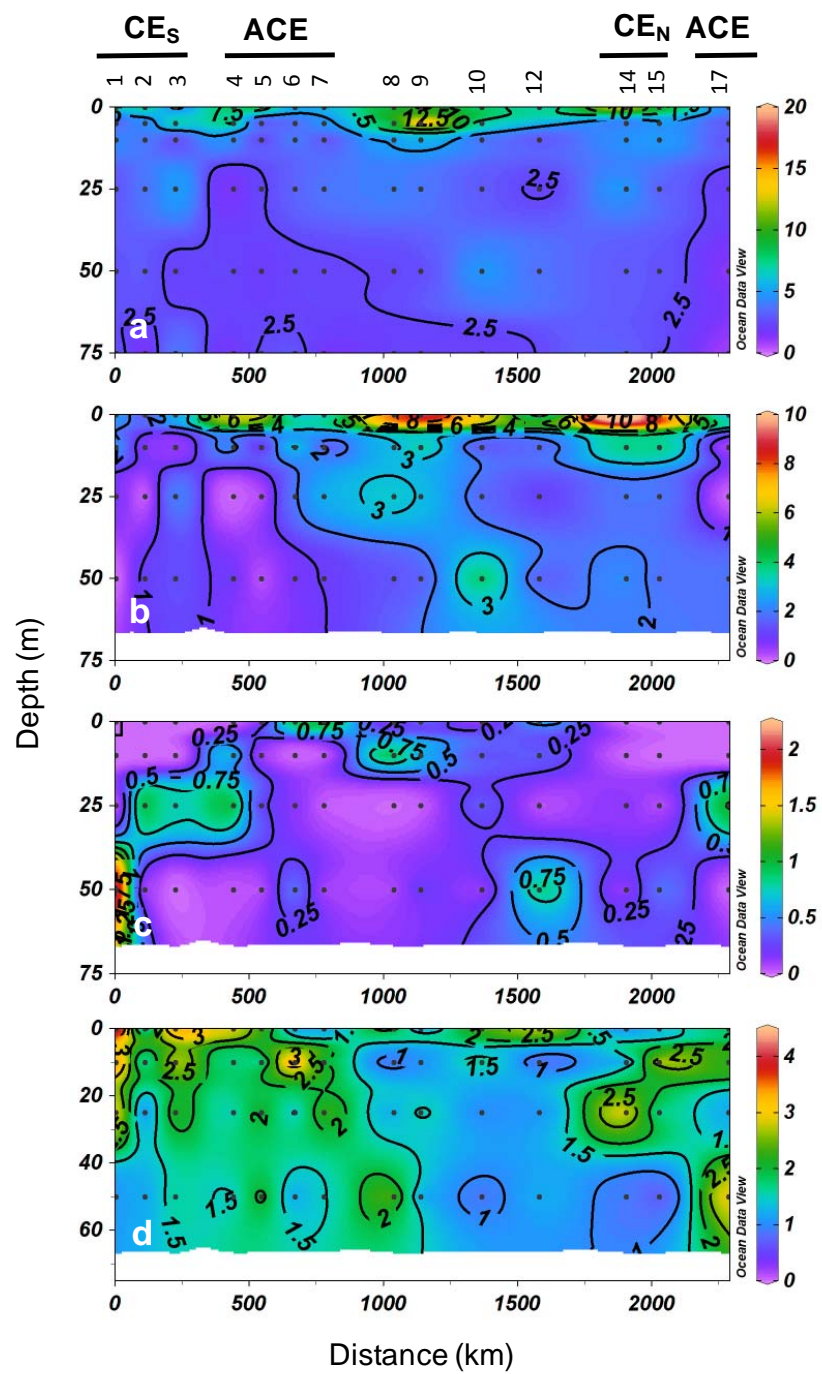


Figure 7

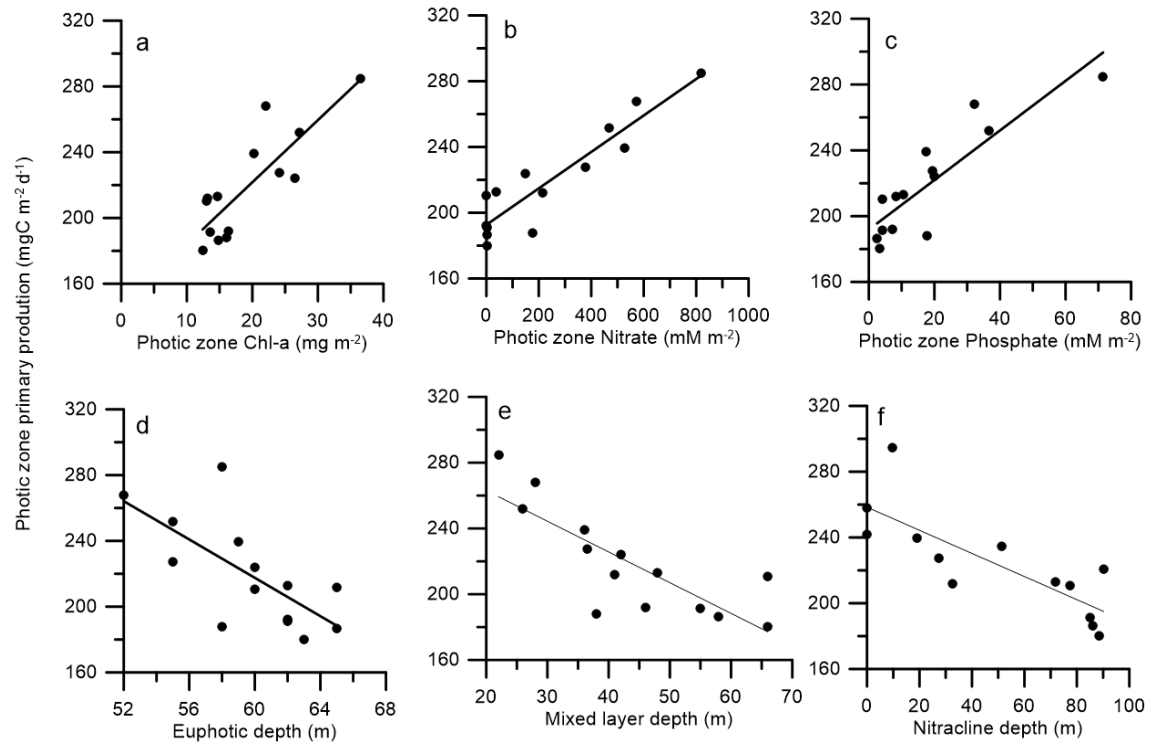
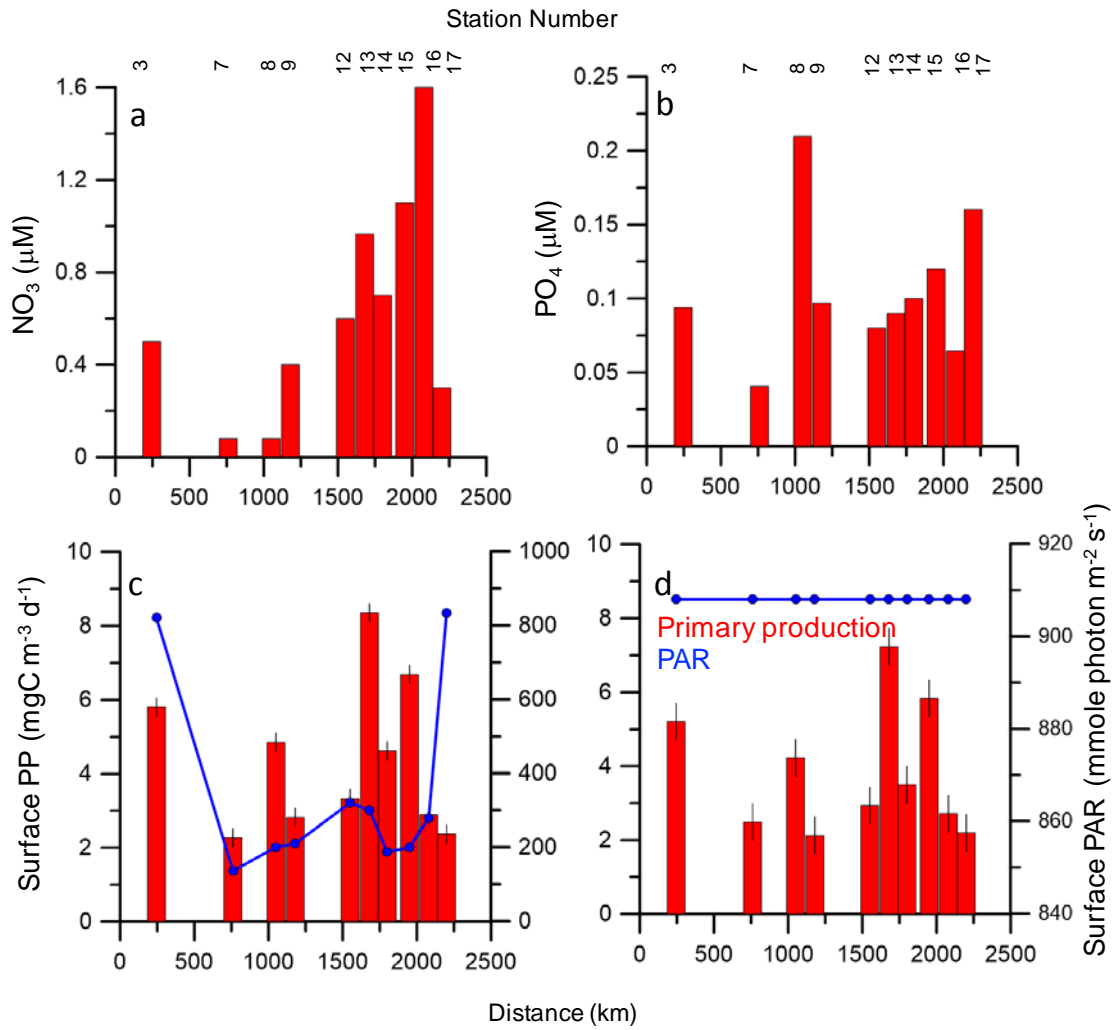
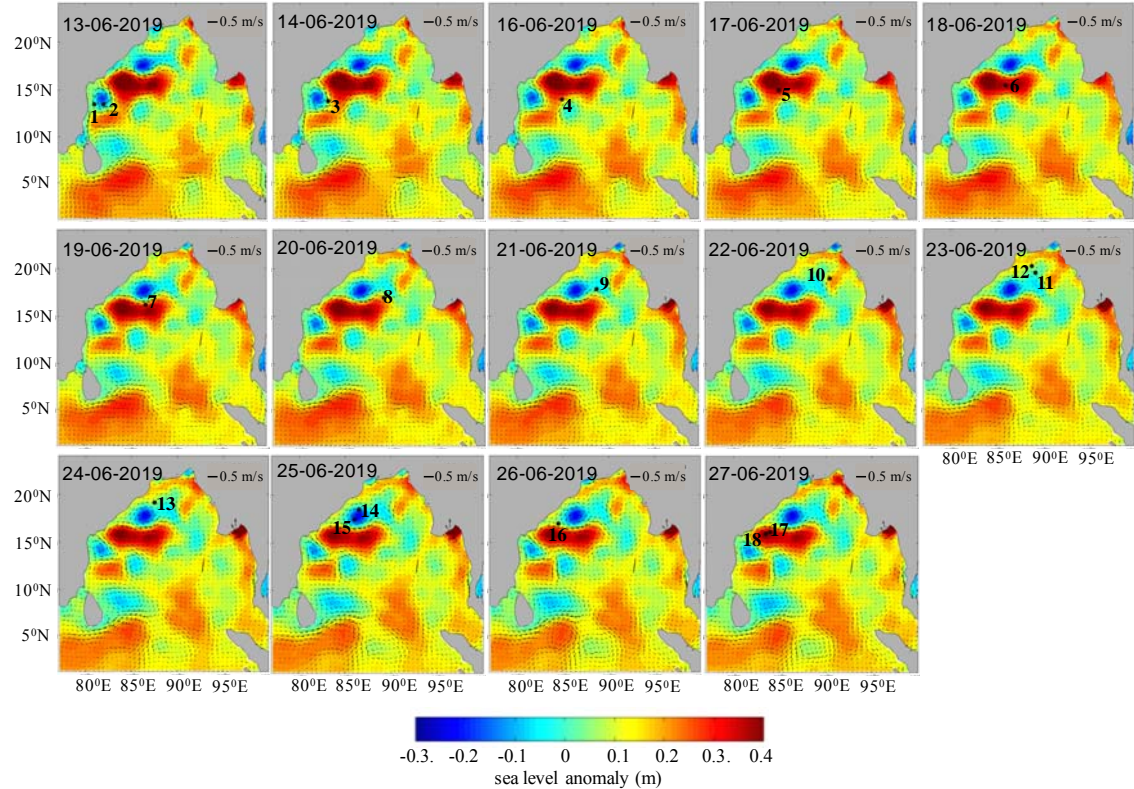


Figure 8



Supplementary Figure S1: The SLA and surface circulation variations on the day of each station collection is depicted and black dot represents the station location and number represent the station number. Vectors denotes the direction and speed of the geostrophic currents at the surface.



Supplementary Figure S2: Mean vertical variations in physical and biogeochemical parameters in the ACE (red), CE (blue) and NE (black) regions.

